



AN EXPLORATION OF THE FREQUENCY DEPENDENCE  
OF MODULATION BLOWUP IN  $\bar{p}p$  COLLIDING BEAMS

D. Neuffer, A. Riddiford, and A. G. Ruggiero

November 1982

An Exploration of the Frequency Dependence  
of Modulation Blowup in  $\bar{p}p$  Colliding Beams

D. Neuffer, A. Riddiford, and A.G. Ruggiero

Abstract

The dependence of beam blow-up in  $\bar{p}p$  colliding beams with tune modulation upon the modulation frequency has been explored with a computer simulation. It is determined that a threshold frequency  $\nu_{TH}$  exists; modulations at frequencies greater than  $\nu_{TH}$  do not lead to beam blow-up. The relationship between this threshold and colliding beams parameters is discussed.

### Introduction

In a previous paper, we had noted that computer simulations of weak-strong  $\bar{p}p$  collisions show the possibility of beam blow-up at large modulation amplitudes. In this paper we report results of an investigation of the dependence of this blow-up upon the modulation frequency, with the modulation amplitude fixed.

The basic features of our simulations of the beam-beam interaction have been described previously,<sup>1</sup> and we will only summarize these briefly in the present paper. Particle transport around an accelerator ring is simulated as the product of two transformations: linear transport around the rings represented by a "Courant-Snyder"<sup>2</sup> (C-S) matrix with the C-S parameters  $\beta_x, \beta_y$  and tunes  $\nu_x, \nu_y$ ; and a nonlinear beam-beam kick determined by assuming a "zero-length" - "weak-strong" interaction with a round gaussian "strong" beam, with the strength of the interaction determined by the "beam-beam tune shift"  $\Delta\nu$ .  $\Delta\nu = .01$  is used in this paper, a large but possible value for  $\bar{p}p$  collisions.

Tune modulation is simulated by changing the tunes  $\nu_x$  and  $\nu_y$  from turn to turn following

$$\nu_x = \nu_{x0} + a_x \sin w_x t$$

$$\nu_y = \nu_{y0} + a_y \sin w_y t$$

with  $w_x = w_y = 2\pi/Nm$ , where  $Nm$  is the modulation period in number of turns, and where  $t = N-1$ ,  $N =$  turn number  $N = 1, 2, 3, \dots$ . In the previous paper,<sup>1</sup>  $\nu_{x0} = .3439$ ,  $\nu_{y0} = .1772$  was chosen, a "resonance-free" case with long-time stability.<sup>3</sup> The parameters  $a_x$  and  $a_y$  were varied and  $Nm$  was set at 1000, a

modulation period expected at  $\bar{p}$  colliders. A large modulational blow-up was noted for the cases  $a_x = -a_y$ ,  $a_x > .004$ , where the modulation carries the beam across low-order resonances (3rd and 6th order).

In the present paper we fix  $v_{x0}$  and  $v_{y0}$  at the same values (.3439, .1772) and fix  $a_x = -a_y = .005$ , a case known to have modulational blow-up at  $Nm = 1000$ , and vary  $Nm$  from  $Nm = 3$  to  $Nm = 100,000$ . Figure 1 shows the time space swept by the modulation in this case, showing the low order resonances which are crossed.

#### Simulation Procedure

In our analysis of stability of particle motion two types of simulations have been used: "long-time" simulations and "reversibility tests". These have previously been described in some detail<sup>1,3,4</sup> and are briefly described below.

In a "long-time" simulation 100 initial particle positions are chosen randomly within a 4-D phase space gaussian distribution, and trajectories generated from these initial conditions are tracked for millions of turns of the storage ring. In the present paper 3 million turn long-time simulations were generated in each case, corresponding to 1 minute of beam storage in the Tevatron I. RMS  $x, y,$  and  $r$  emittances ( $\epsilon_x, \epsilon_y$  and  $\epsilon_r = \epsilon_x^2 + \epsilon_y^2$ ) for the 100 particle ensemble were calculated every 2000 turns after the first thousand turns and changes in these values were monitored. "Doubling times" are calculated from these emittance values from a least squares fit, which obtains a slope or rate of increase (decrease) of these values. The "doubling time" is the average emittance divided by this slope, so a short doubling time indicates beam blow-up.

Individual particle trajectories are also monitored for significant amplitude changes.

In previous simulations of modulational beam blow-up, the blow-up was associated with the appearance of "chaotic" trajectories, where a "chaotic" trajectory is a particle trajectory which diverges exponentially in time from nearby trajectories in phase space. "Reversibility" tests are performed to detect these trajectories. In these tests trajectories are tracked forward 100,000 turns and returned by reversing the transformations, and forward and return positions are compared. "Chaotic" trajectories develop deviations exponentially and, in these cases, can accumulate errors of order unity in 100,000 turns. "Non-chaotic" cases develop errors linearly, and, in our double precision tests, develop errors of order  $10^{-20}$ . A clear empirical separation between these two types is obtained.

#### Reversibility Test

Reversibility tests for a set of 100 particles were run for  $N_m = 8, 16, 32, 64, 100, 200, 400, 800, 1000, 2000, 4000, 10,000$  and  $100,000$ . For  $N_m \leq 10,000$ , the tests included 100,000 forward and return turns. For  $N_m = 100,000$  ten periods were tracked (1,000,000 turns). In each test trajectories were classified as chaotic when the error over the full test length exceeded  $10^{-10}$ . The results of these repeatability tests are summarized in Table I.

A gradual increase in the number of chaotic trajectories from zero for  $N_m = 16$  can be seen with a maximum of  $\sqrt{50}$  (out of 100) for  $N_m \geq 300$ . The number appears to remain constant or decrease very slowly for larger  $N_m$

(low modulation frequency). This is illustrated graphically in Figure 2.

A complementary behavior can be seen in the behavior of the Liapunov exponents of the trajectories. The Liapunov exponent is the factor  $A$  which appears in the error growth equation

$$\Delta = \Delta_0 e^{AN}$$

where  $\Delta_0$  is an initial error and  $\Delta$  is the exponentially enhanced error at turn  $N$ . For  $Nm = 2000$ ,  $A$  does not show any significant dependence on  $Nm$  for those trajectories that are chaotic with  $A \approx 1.0 \times 10^{-3}$  on average. For  $Nm > 2000$  a noticeable decrease in  $A$  occurs, with  $A \approx 10^{-4}$  for  $Nm = 10,000$  and  $A \approx 10^{-5}$  for  $Nm = 100,000$ , apparently approaching a  $\sim 1/Nm$  dependence. This behavior is displayed graphically in Figure 3.

#### "Long-Time" Simulation Results

We have completed "long-time" simulations for values of  $Nm = 8$  to  $Nm = 100,000$ . These simulations included  $> 3$  million turns (1 minute Tevatron time). The results are summarized in Table II, where mean emittance values and "doubling times" are tabulated.

The mean emittance values  $\bar{\epsilon}_x$ ,  $\bar{\epsilon}_y$  are averaged over the 200,000 turns previous to the indicated turn numbers ( $N = 0.2, 1., 3.$  million) where measurements of  $\bar{\epsilon}$  for the 100-particle ensemble are taken every 2000 turns. The "doubling times"  $T$  are found from the inverse of the slope of a least squares fit to  $\epsilon_x$ ,  $\epsilon_y$ ,  $\epsilon_r = \sqrt{\epsilon_x^2 + \epsilon_y^2}$  as a function of time; that is

$$\epsilon_x = \bar{\epsilon}_{x_0} + \frac{AN}{N_0} \quad \text{and} \quad T_x = \frac{\bar{\epsilon}_x}{A} \quad \text{minutes}$$

where  $N_D = 3$  million turns = 1 minute real time.

All emittance values measured before the indicated turn number are included in the doubling time estimates. Note that a negative doubling time indicates a decreasing emittance.

These doubling times can be compared to "statistically significant" doubling times  $T_\sigma$  is found from the statistical error  $\sigma$  in the slope A:

$$T_\sigma = \bar{\epsilon} / \sigma$$

In the tables,  $S_R$ , the ratio between the statistically significant doubling time and the radial double time is displayed:

$$S_R = \frac{T_{\sigma_R y}}{T_R} = \frac{A_R}{\sigma_R}$$

When  $S_R$  is sufficiently larger than 1, a statistically significant change in beam emittances is indicated. Similar comparisons for x and y emittances have been made but are not explicitly included in Table 2. A reasonable estimate can be obtained from symmetry by noting

$$T_{\sigma_x} \sim T_\sigma \sim T_{\sigma_R}$$

from which  $S_x$  and  $S_y$  can be deduced.

Table II shows that for  $Nm \leq 100$ , no significant increases in total beam emittances are observed; extrapolated doubling times are many hours. For  $Nm = 200$  significant increases appear and for  $Nm > 400$  fast beam blow-up occurs with doubling times of several seconds.

For  $N_m \gtrsim 10,000$  a noticeable decrease in the calculated 200,000 turn doubling times can be observed, following the  $1/N_m$  dependence noted in the observations of Liapunov exponent, described above.

This behavior is displayed graphically in Figure 4 where the slope parameter  $\lambda$  as a function of  $N_m$  is plotted. They show a "threshold" dependence with increasing  $N_m$ . At  $N_m = 200$ , 3 "divergent" trajectories appear. The number increases with  $N_m$  to an approximately constant value of 30 for  $N_m \sim 1000$  and decreases again for  $N_m > 1000$ .

#### Discussion of Modulational Beam Blow-Up

This study of the frequency dependence of modulational blow-up provides information which can be used in constructing a theoretical model to describe that blow-up. From this paper and reference 1, we note that beam blow-up can occur when a low order resonance is swept across the beam, provided the "speed of sweeping" (modulation frequency) is not "too fast" and not "too slow". The resonance is mostly seen when the modulation frequency is comparable with the precession frequency of the trajectory in the resonance island region.

In our case, as we can see by inspecting Figure 1, there are two resonances which are actually involved in the sweeping.

Investigation of individual particle trajectories show that they can be classified into three groups:

1. Non-chaotic trajectories; these do not change amplitude significantly.

2. "Non-divergent" "chaotic" trajectories which remain confined to amplitudes near their original values.
3. "Divergent" chaotic trajectories, those which change amplitudes greatly in the 3 million turn simulations. These trajectories participate in the beam blow-up for  $Nm > 200$ .

In Figure 2 and Table I we indicate the number of these divergent chaotic trajectories. We can clearly note a strong correlation between the appearance of this last kind of particles and beam growth.

In Figure 5 we show the location of the particles in the tune diagrams. It corresponds to the case  $Nm = 300$ . The betatron tune values are those obtained by averaging over the first 800 turns of the simulation. We also show in the same figure the location of the two major resonance when they are the most inside into the beam. Reversibility test and emittance growth measurements were done after 6 million turns. The particles, (A) that are not swept by the two resonances are stable and meet the reversibility test positively. The non-reversible particles that also grow to large emittance values (F) are swept by the two resonance lines. Chaotic particles (C) which do not grow in amplitude are confined in a region between the (A) and (F) particles.

In Figure 6 we show the same distribution 6 million turns later. The (F) particles have been pushed to larger amplitude. These particles are those initially at large amplitude and are those that are chaotic and grow. This is in agreement with some observations of the beam-beam effect in the SPS in CERN with proton and antiproton beams colliding.<sup>5</sup>

## References

1. D. Neuffer, A. Riddiford, and A.G. Ruggiero, FN-359, Fermilab, Feb. 1982.
2. E.D. Courant and H.S. Snyder, *Annals of Physics* 3, 1 (1958).
3. D. Neuffer, A. Riddiford, and A.G. Ruggiero, FN-346, Fermilab, Oct. 1981.
4. D. Neuffer, A. Riddiford, and A.G. Ruggiero, FN-363, Fermilab, March 1982.
5. L. Evans, Private Communication, Summer 1982.

Table I Results of Repeatability Tests

Nm	Number of Chaotic Trajectories (out of 100 total)	Number of Trajectories which diverge to large amplitude
8	0	0
16	0	0
32	10	0
64	7	0
100	5	0
200	13	3
400	28	18
<b>600</b>	<b>29</b>	<b>-</b>
<b>800</b>	<b>40</b>	<b>27</b>
1000	41	-
2000	50	24
4000	46	22
10,000	42	18
100,000	39	7

Table II Long Time Simulation ResultsCase I: Nm = 8

Turn Number (millions)	$\bar{\varepsilon}_x$ (mm-mr)	$\bar{\varepsilon}_y$ (mm-mr)	$T_x$ Doubling Times	$T_y$ Doubling Times	$T_R$ (days)	$S_R$
0.2	.01755	.01878	-.005	.005	.04	0.38
1.0	.01752	.01883	0.071	.085	-4.63	0.036
3.0	.01752	.01882	2.55	1.06	1.49	0.565

Case II: Nm = 32

$N_T$ (M)	$\bar{\varepsilon}_x$ (mm-mr)	$\bar{\varepsilon}_y$ (mm-mr)	$T_x$ (hours)	$T_y$ (hours)	$T_R$	$S_R$
0.2	.01762	.01894	.083	.278	.133	2.94
1.0	.01777	.01882	.688	-.928	9.30	0.42
3.0	.01791	.01876	1.06	-.928	10.1	2.19
5.0	.01779	.01888	7.4	-17.5	30.0	1.45

Case III: Nm = 64

$N_T$ (M)	$\bar{\varepsilon}_x$ (mm-mr)	$\bar{\varepsilon}_y$ (mm-mr)	$T_x$ (hours)	$T_y$ (hours)	$T_R$	$S_R$
0.2	.01740	.01906	-.59	.36	1.35	0.26
1.0	.01745	.01891	35.8	-.78	-1.48	2.56
3.0	.01748	.01889	-8.1	22.4	-31.0	0.63

Case IV: Nm = 100

$N_T$ (M)	$\bar{\varepsilon}_x$ (mm-mr)	$\bar{\varepsilon}_y$ (mm-mr)	$T_x$ (hours)	$T_y$ (hours)	$T_R$	$S_R$
0.2	.01731	.01914	-0.48	0.10	0.19	1.85
1.0	.01734	.01904	1.32	-0.77	2.74	1.35
3.0	.01743	.01906	4.30	-4.39	51.6	0.37

Case V: Nm = 200

$N_T$ (M)	$\epsilon_y$ (mm-mr)	$\epsilon_y$ (mm-mr)	$T_x$	$T_y$ (minutes)	$T_R$	$S_R$
0.2	.01779	.01880	13.2	-1.42	-2.97	6.9
1.0	.01889	.01934	4.6	6.4	5.36	19.4
3.0	.02011	.02091	6.8	9.0	7.71	84.0

Case VI: Nm = 400

$N_T$ (M)	$\epsilon_x$ (mm-mr)	$\epsilon_y$ (mm-mr)	$T_x$	$T_y$ (seconds)	$T_R$	$S_R$
0.2	.02347	.02333	7.8	10.4	8.8	46.
1.0	.05540	.03664	20.2	35.9	24.2	108.
3.0	.07003	.06560	77.6	59.7	69.6	127.

Case VII: Nm = 800

$N_T$ (M)	$\epsilon_x$ (mm-mr)	$\epsilon_y$ (mm-mr)	$T_x$	$T_y$ (seconds)	$T_R$	$S_R$
0.2	.02739	.02535	4.8	10.6	6.4	46.
1.0	.05137	.07967	32.3	15.7	19.5	70.
3.0	.08193	.10930	80.	59.	64.	96.

Case VIII: Nm = 2000

$N_T$ (M)	$\epsilon_x$ (mm-mr)	$\epsilon_y$ (mm-mr)	$T_x$	$T_y$ (seconds)	$T_R$	$S_R$
0.2	.02594	.03051	5.7	4.4	4.8	38.
1.0	.07269	.06938	13.4	14.0	13.7	194.
3.0	.1184	.1553	48.6	40.1	43.3	187.

Case IX: Nm = 4000

$N_T$ (M)	$\epsilon_x$ (mm-mr)	$\epsilon_y$ (mm-mr)	$T_x$	$T_y$ (seconds)	$T_R$	$S_R$
0.2	.02838	.02942	4.6	4.8	4.7	45.
1.0	.08313	.1143	15.4	10.3	11.7	136.
3.0	.1445	.2285	48.2	43.0	44.7	121.

Case X: Nm = 10,000

$N_T$ (M)	$\bar{\epsilon}_x$ (mm-mr)	$\bar{\epsilon}_y$ (mm-mr)	$T_x$ (seconds)	$T_y$ (seconds)	$T_R$	$S_R$
0.2	0.02762	0.03243	5.7	3.7	4.3	5.1
1.0	0.08577	0.08065	11.1	13.9	12.3	163.
3.0	0.21976	0.25361	38.4	32.7	35.1	361.

Case XI: Nm = 100,000

$N_T$ (M)	$\bar{\epsilon}_x$ (mm-mr)	$\bar{\epsilon}_y$ (mm-mr)	$T_x$ (seconds)	$T_y$ (seconds)	$T_R$	$S_R$
0.2	0.01875	0.01876	20.8	68.8	30.4	16.
1.0	0.02961	0.02622	17.9	27.4	20.9	70.
3.0	0.06862	0.05353	37.8	43.0	39.8	108.

Figure 1 Area of tune space swept out by

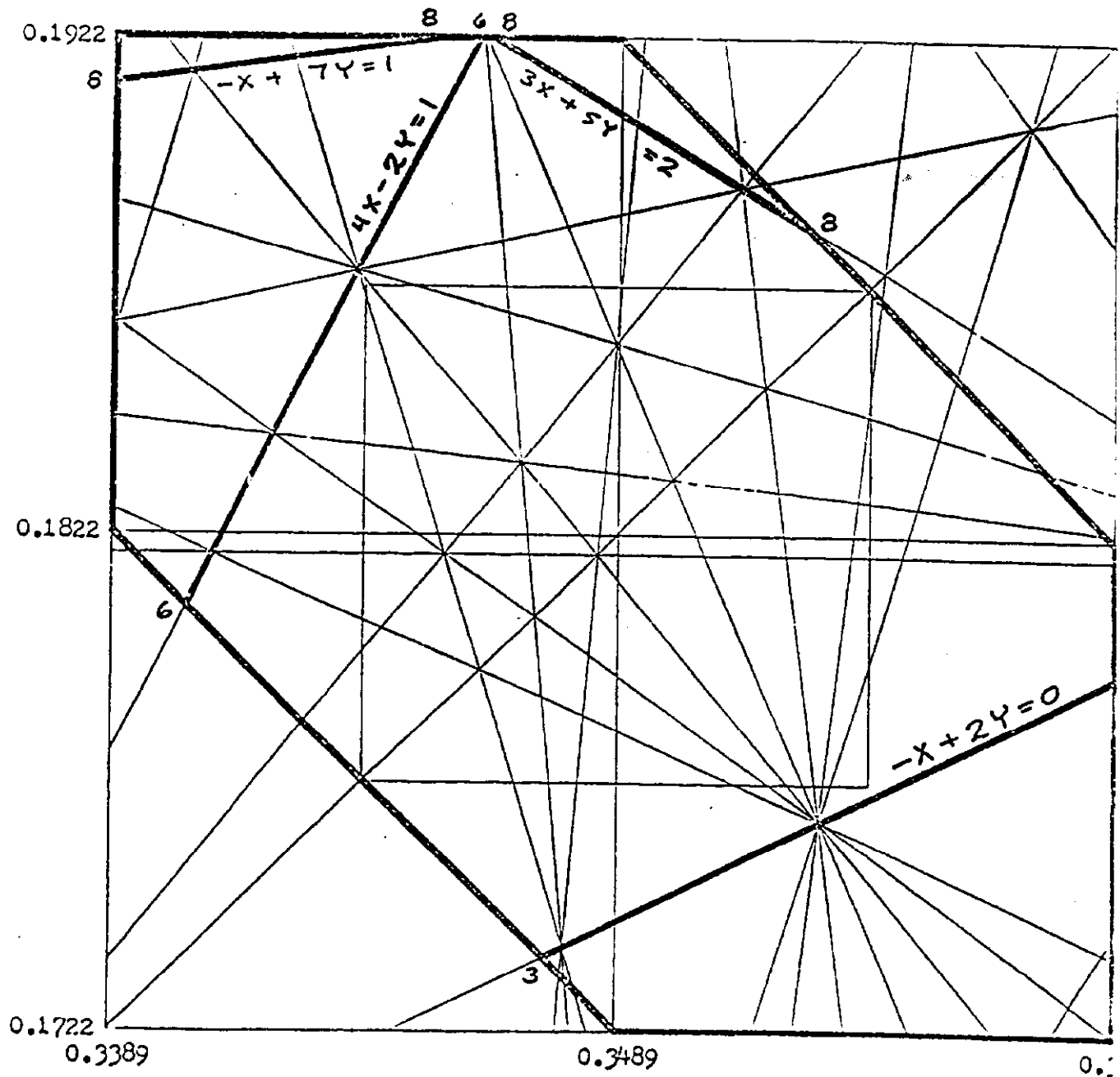
Case C-.005:  $v_x = 0.3439 + 0.005 \sin \theta$

$v_y = 0.1772 - 0.005 \sin \theta$

$\Delta v = 0.01$

$\theta = 2\pi(n-1)/1000$

n = turn number



Reversibility test results; 100,000 turns forward, 100,000 turns reverse  
 (except  $10^6$  forward and  $10^6$  back for NCYCLE = 100,000).

$$\mu_x/2\pi = 0.3539 + 0.005 \sin(2\pi N/NCYCLE)$$

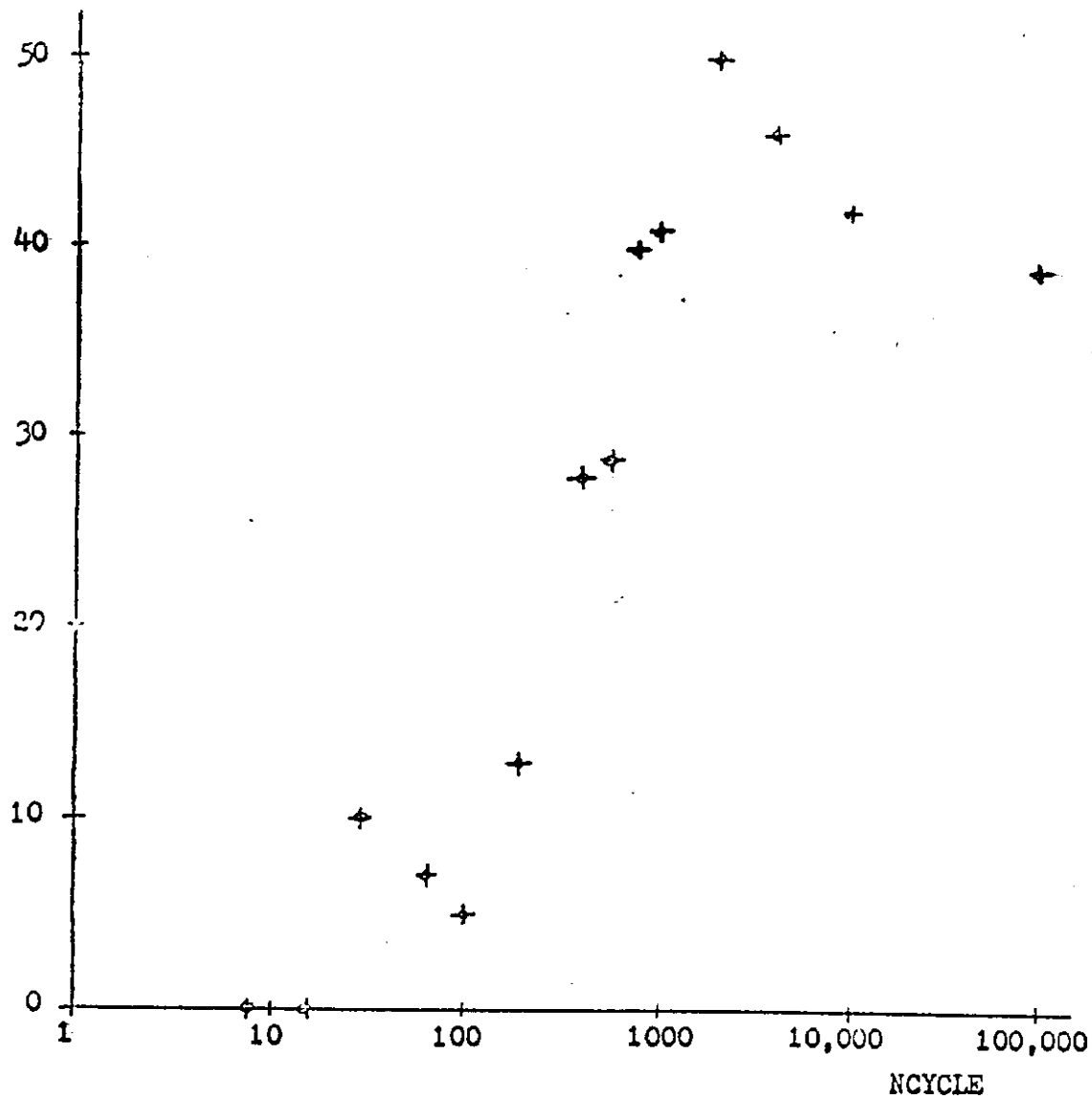
N = Turn number

$$\mu_y/2\pi = 0.1872 - 0.005 \sin(2\pi N/NCYCLE)$$

= 0, 1, 2, ...

$$GX = GY = 2\pi\Delta\gamma, \quad \Delta\gamma = 0.01$$

Number  
of  
failed  
particles



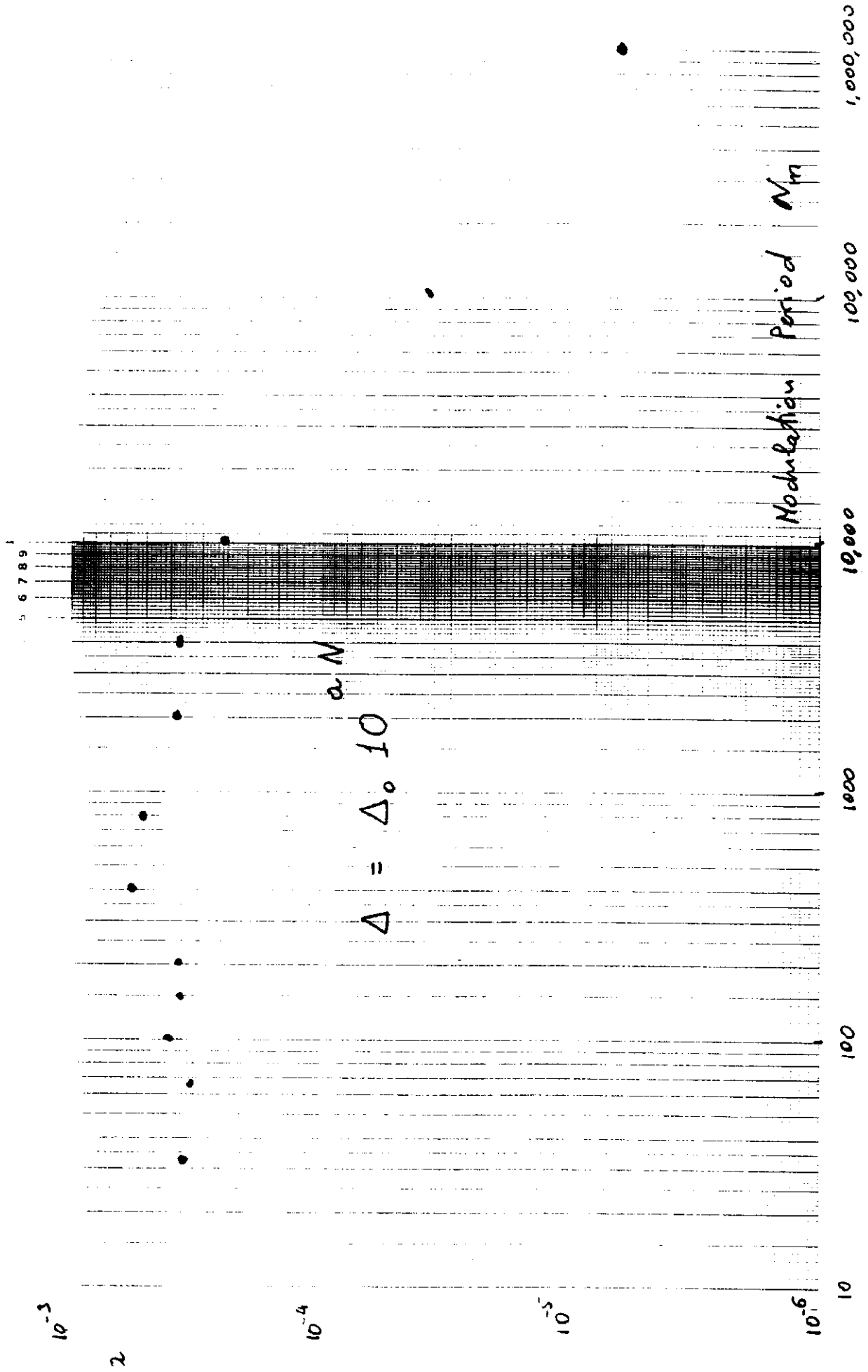


Fig. 3. Average Lyapunov exponent as function of modulation period

Figure 4

Slopes after 200,000 turns.

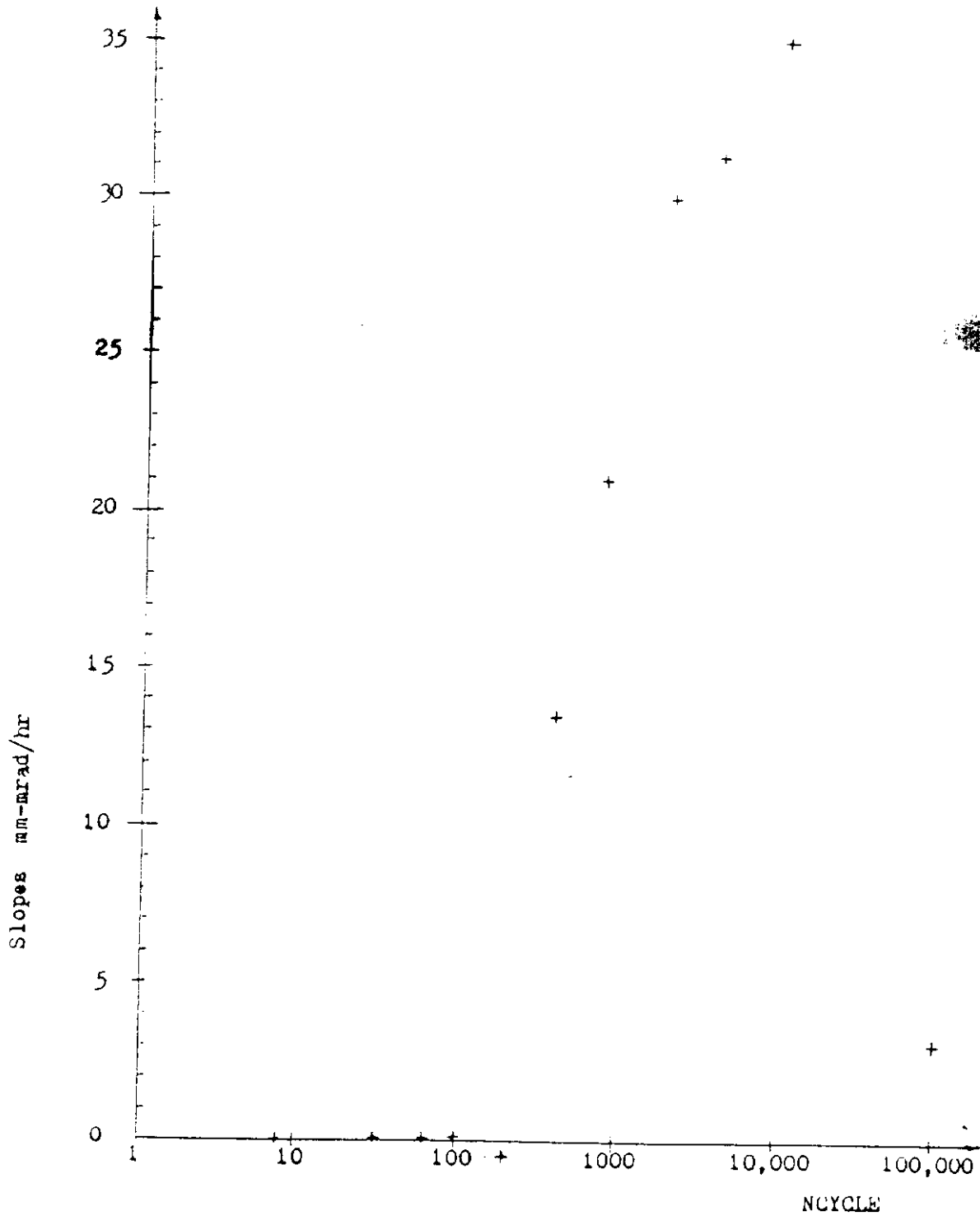
$$\mu_x/2\pi = 0.3539 + 0.005 \sin(2\pi N/\text{NCYCLE})$$

$$\mu_y/2\pi = 0.1672 - 0.005 \sin(2\pi N/\text{NCYCLE})$$

$$GX = GY = 2\pi\Delta\nu, \quad \Delta\nu = 0.01$$

$N$  = Turn number

= 0, 1, 2, ...



Tunes averaged over turns 0 to 800. NCYCLE = 800.

$$\mu_x/2\pi = 0.3539 + 0.005 \sin \theta \quad \theta = 2\pi N/800, N = \text{Turn number.}$$

$$\mu_y/2\pi = 0.1572 - 0.005 \sin \theta \quad GX = GY = 2\pi \Delta\nu, \Delta\nu = 0.01$$

The lower-left corner corresponds with  $\mu_x/2\pi - \Delta\nu, \mu_y/2\pi - \Delta\nu$ .

The upper-right corner corresponds with  $\mu_x/2\pi, \mu_y/2\pi$ .

- Labels: A Reversible and small emittance after 3 million turns.  
 C Chaotic and small emittance after 3 million turns.  
 F Chaotic and large emittance after 3 million turns.  
 N Reversible and large emittance after 3 million turns.

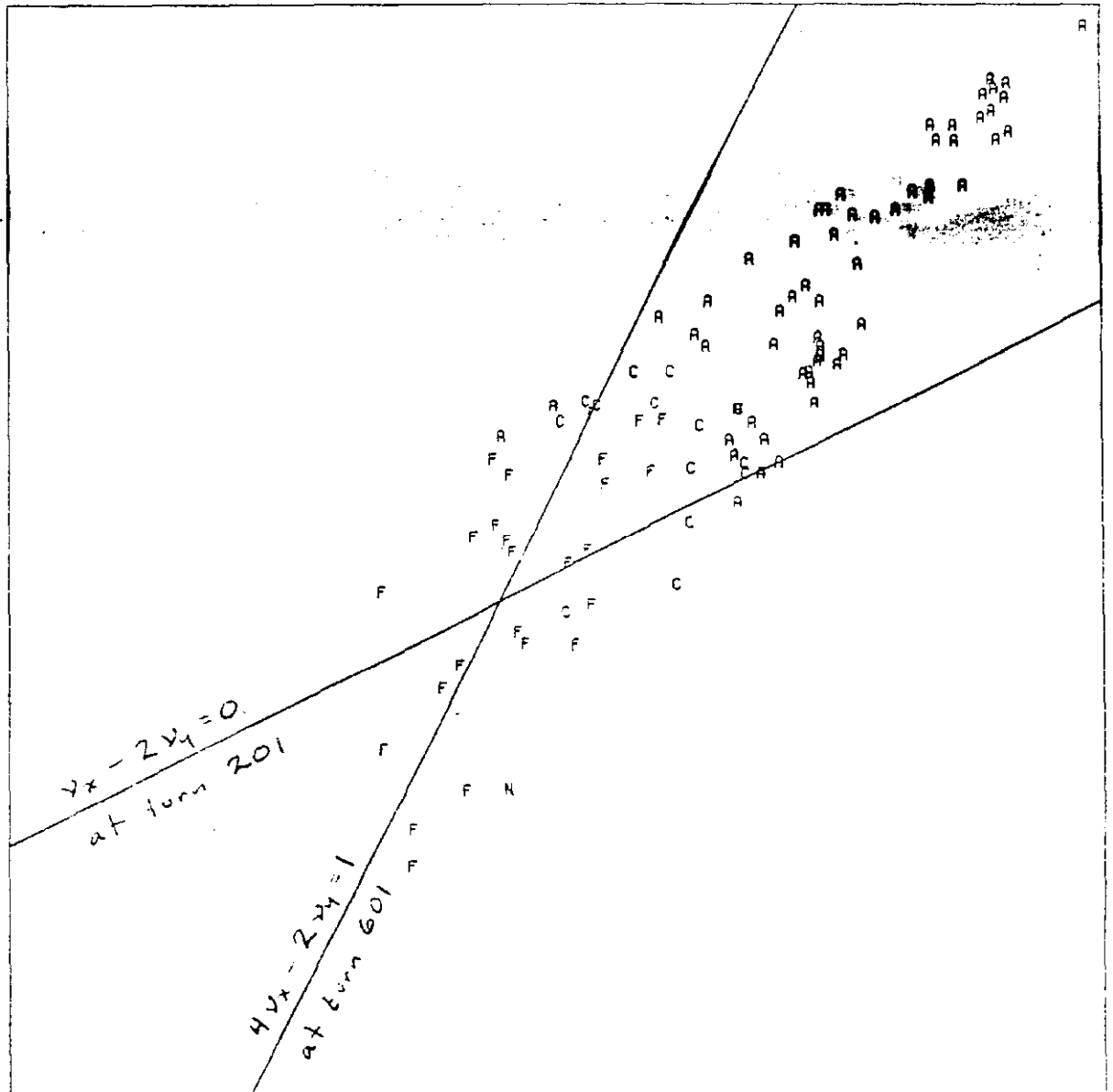


Figure 6

Tunes averaged over turns 3,000,000 to 3,000,800. NCYCLE = 800.

$$\mu_x/2\pi = 0.3539 + 0.005 \sin\theta \quad \theta = 2\pi N/800, N = \text{Turn number.}$$

$$\mu_y/2\pi = 0.1372 - 0.005 \sin\theta \quad GX = GY = 2\pi\Delta\nu, \Delta\nu = 0.01$$

The lower-left corner corresponds with  $\mu_x/2\pi - \Delta\nu, \mu_y/2\pi - \Delta\nu$ .

The upper-right corner corresponds with  $\mu_x/2\pi, \mu_y/2\pi$ .

- Labels: A Reversible and small emittance after 3 million turns.  
 C Chaotic and small emittance after 3 million turns.  
 F Chaotic and large emittance after 3 million turns.  
 N Reversible and large emittance after 3 million turns.

